The consequences of different printing chamber temperatures in extrusion-based additive manufacturing

Spoerk Martin*[a,b)], Arbeiter Florian[c)], Raguž Ivan[a)], Traxler Gerhard[d)], Schuschnigg Stephan[a)], Cardon Ludwig[b)], Holzer Clemens[a)]

[a)]*Polymer Processing, Montanuniversitaet Leoben, Otto Gloeckel-Straße 2, 8700 Leoben, Austria*

[b)]*Centre for Polymer and Material Technologies, Department of Materials, Textiles and Chemical Engineering, Ghent University, Technologiepark 915, 9052 Zwijnaarde, Belgium*

[c)]*Materials Science and Testing of Polymers, Montanuniversitaet Leoben, Otto Gloeckel-Straße 2, 8700 Leoben, Austria*

[d)]*Machine Vision, Profactor GmbH, Graumanngasse 7, C3, 1150 Wien, Austria*

[*)]*Corresponding author: martin.spoerk@unileoben.ac.at*

ABSTRACT: Materials that are processed by means of extrusion-based additive manufacturing are exposed to complex temperature conditions during manufacturing, resulting from quick temperature alterations due to the moving nozzle. Consequently, a rather inhomogeneous temperature distribution is present in the printing chamber, which can intensify issues such as high internal stresses, unintentional crystal growth and undesired part deformations. This study aims at tackling these problems by investigating the consequences of increased printing chamber temperatures on 3D-printed polypropylene (PP). In-situ thermography measurements during printing revealed a drastic decrease in the temperature fluctuations as soon as parts are printed at a controlled increased chamber temperature, leading to a more homogeneous temperature distribution. As a result, internal stresses declined and the warpage of printed parts considerably decreased compared to the conventionally used surrounding room temperature. Since the maxima of the strand temperatures easily surpass 100 °C for a chamber temperature of 55 °C, the crystal modification partly changed from α-PP to β-PP, which was confirmed by thermograms and X-ray diffraction. As the mean strand temperatures during printing are in the close proximity of the temperature of the maximum crystal growth rate of PP, fewer and bigger, but more homogeneous spherulites were formed. Additionally, shish-kebab structures tended to form at high chamber temperatures due to strong process orientations. The found crystallographic changes introduced by changes in the printing chamber temperature can be employed to tailor the material properties of 3D-printed PP. The proposed strategy can act as the foundation for similar studies on other printable semi-crystalline polymers.

1 INTRODUCTION

Extrusion-based additive manufacturing, also known as fused filament fabrication (FFF) is a promising, novel processing technology that enables the production of complex, three-dimensional parts by the selective deposition of thermoplastics and a layer-by-layer fabrication [1]. Polypropylene (PP) is a material that has nearly been neglected for FFF due to the processes' complex temperature conditions, the material's high crystallinity and in turn its high tendency to warp [2]. This material, though, exhibits favourable properties that can hardly be achieved by other commercially available FFF materials, such as low cost and density, high impact strength, chemical resistance and moisture stability [3]. Apart from the incorporation of fillers to the PP matrix [4], it was shown for acrylonitrile butadiene styrene (ABS) that changes in the processing conditions, such as the printing chamber temperature T_{Ch}, can significantly improve the warpage and mechanical properties [5, 6]. An increased T_{Ch}, for instance, can homogenise the complex temperature conditions during printing that are caused by the rapid heating and cooling of the material by the moving nozzle [7]. Consequently, internal stresses can be reduced and a more controlled crystal growth might be allowed [8]. Additionally, it was found that very high T_{Ch} can even alter the crystalline morphology of polymers during FFF [9]. Recently, a previous study by the authors [6] confirmed and expanded these findings for 3D-printed PP by detailed investigations on the consequences of an increased T_{Ch} on the warpage, mechanical, morphological and thermal properties.

The present article gives an overview of the consequences of different T_{Ch} on selective topics. It is based on the recently published article [6] and is complemented by additional unpublished characterisation techniques. The focus of the present work lies on the effect of the T_{Ch} on microscopic properties that in turn are responsible for the previously described changes in warpage and mechanical properties.

2 EXPERIMENTAL

2.1 *Specimen preparation*

A polypropylene heterophasic copolymer (PP, Borealis AG, Austria) was processed to filaments in the single screw extruder FT-E20T-MP-IS (Dr. Collin GmbH, Germany) at 185 °C, a screw speed of 30 rpm, through a die of 1.9 mm diameter and 25.05 mm length and a water bath. Before spooling the filament, its diameter was recorded by a Sikora Laser 2010T (Sikora AG, Germany) diameter measurement device. The filament was processed by a Duplicator i3 v2 (Wanhao, China) FFF printer with a steel nozzle of 0.6 mm in diameter. Unless stated otherwise, Charpy specimens (80×10×4 mm^3) were sliced in a unidirectional orientation (0° printing orientation) with the software Simplify3D Version 3.0 (Simplify3D, USA). The detailed printing parameters are summarised in Ref. [6]. Apart from printing at a surrounding and platform temperature of room temperature, the printing chamber was increased to a T_{Ch} of 55 °C by insulating the FFF-printer with expanded polystyrene plates and increasing the platform to 70 °C. In order not to lead to failure of essential machine components of the FFF printer, prints at a T_{Ch} higher than 55 °C were not conducted.

During the preparation of the printed Charpy specimens, the temperature of a fixed position on the contour-strand of the first specimen in the third printing layer was recorded by means of the thermal camera Silver450 (Cedip Infrared Systems, France) equipped with a lens of a focal length of 27 mm in order to estimate the temperature in the specimen during processing. For details on the test set-up, please refer to Ref. [6].

2.2 *Polarised optical microscopy*

Thin slices of 20 µm were cut from the middle of untested printed Charpy specimens by the Leica RM 2255 (Leica Microsystems GmbH, Germany) microtome. The slices were analysed in the optical microscope Olympus SZX12 (Olympus Life Science Europe GmbH, Germany) under transmitted light and a polariser.

2.3 *Thermal analysis*

The melting behaviour of similar sliced pieces, cut 20 mm off the edge of an untested Charpy specimen and each having a mass of 10±1 mg, was investigated using the differential scanning calorimeter (DSC) DSC 1 (Mettler Toledo GmbH, Switzerland) under nitrogen atmosphere. Seven samples per setting were analysed between 25 °C and 200 °C, in which every sample was exposed to heat-cool-heat runs with a heating and cooling rate of 10 $K \cdot min^{-1}$.

2.4 *X-ray diffraction*

To further investigate the crystalline structure of the thin-sliced samples of untested printed Charpy specimens, in-situ X-ray diffraction (XRD) measurements were performed on a Bruker D8 Discover XRD, a Cu X-ray source and a linear detector (Bruker Corporation, USA). $\theta-2\theta$ measurements between 5 and 55° were carried out at atmospheric pressure in reflection mode. The samples, fixed to a silicon sample cup, were exposed to heat-cool runs with the same settings as for the DSC. The temperature was measured with a K-type thermocouple and during heating/cooling the samples were subjected to a controlled Helium flow of 250 sccm.

2.5 *Thermal conductivity*

Thermal conductivity tests were performed on 3D-printed PP plates (30×30×5 mm^3) with different printing orientations (0°, 90°, 0°/90°, ±45°) on the thermal conductivity analyser TPS 2500 S and the Kapton sensor 5465 (both Hot Disk AB, Sweden) according to the standard ISO 22007-2. For detailed information on the methodology and the printing orientations please refer to Ref. [10].

3 RESULTS AND DISCUSSION

It is known that an increased T_{Ch} can have tremendous consequences on both the mechanical and warpage properties of parts produced by extrusion-based additive manufacturing [6]. Apart from a more homogeneous temperature distribution within the printing chamber [6], the key aspects for these positive effects are on a molecular level and will be described in the following.

3.1 *Impact on the spherulite size*

The crystallographic appearance of the welding zone between two adjacent strands seems to be independent on the different T_{Ch}, as both the specimens produced at a T_{Ch} of 25 °C (Figure 1a) and of 55 °C (Figure 1b) consist of comparable fine crystals, similarly to 3D-printed PLA [11] or vibration-welded PP [12]. However, contrary to investigations on additively manufactured PLA [11], the spherulites of the strands themselves differ significantly, as the sample printed at a T_{Ch} of 55 °C exhibits spherulites with double the size (approximately 50 µm) than that produced at a T_{Ch} of 25 °C (roughly 25 µm). The reason for this trend is related to the temperatures that occur over a long period of time during printing and the different crystal growth and nucleation rates of PP at the two T_{Ch}. The in-situ thermography measurements during printing (Figure 1) reveal the answer to this phenomenon. The due to the printing sequence repeatedly occurring temperature peaks (please refer to Ref. [6] for more details),

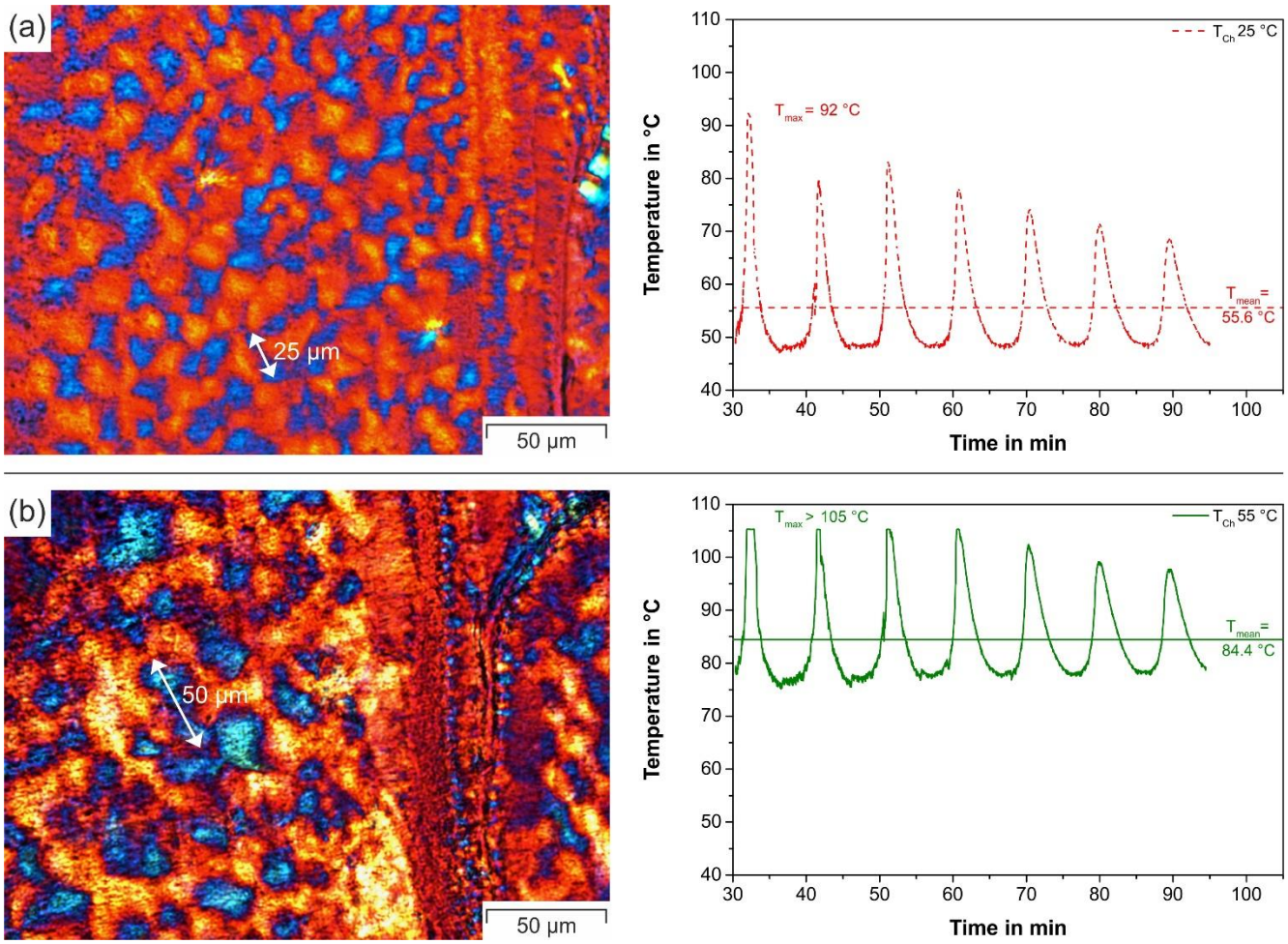

Figure 1: Polarised optical microscopy images of microtome cuts of untested 3D-printed PP Charpy specimens (left) along with the temperature evolution of a contour strand of the third printing layer of a Charpy specimen during one printing cycle (right) for a printing chamber temperature T_{Ch} of 25 °C (a) and 55 °C (b). The microscopy images represent longitudinal strands of one layer. The white arrows show the difference in spherulite diameter. For the temperature evolution, the mean temperatures of the strand in the third layer (T_{mean}) and the maximum temperature (T_{max}), both determined for a time period between the deposition of the investigated strand (30 min) and the completion of the print (95 min) are marked.

show a drastic difference in the mean strand temperature (T_{mean}) over an observation time of 65 min for the two T_{Ch}. The increase of 30 °C in the T_{Ch} also leads to a similar T_{mean} enlargement from 55.6 °C to 84.4 °C. As the latter temperature is close to the temperature of the maximum crystal growth rate of PP (77 °C) [8], and the specimen is exposed to this temperature for a long period of time (overall printing time of 95 min), few nuclei grow at a rather high rate, which results in large spherulites for the specimen processed at a T_{Ch} of 55 °C. On the other hand, the T_{mean} of 55.6 °C is significantly lower than 77 °C, which results in lower crystal growth rates, but higher nucleation rates [8]. Hence, the spherulites of the specimen printed at a T_{Ch} of 25 °C are considerably smaller than that of 55 °C, but they are more numerous [6]. As a result, the specimens with bigger spherulites tend to exhibit a reduced warpage, but also a decreased elongation at break (for details please refer to Ref. [6]).

3.2 *Impact on the crystalline structure*

The processing history during 3D-printing also influences the crystalline structures, which in turn has the potential to improve the toughness of the printed specimens [6]. Compared to the specimens printed at a T_{Ch} of 25 °C, those processed at a T_{Ch} of 55 °C reveal two additional melting peaks in their first melting curve between 145 °C and 160 °C (Figure 2a). After a controlled cooling step (second heating), though, the two samples show nearly an identical melting behaviour. This hints at having a processing induced change in crystalline modification that most certainly is caused by the frequent exposure of the specimen produced at a T_{Ch} of 55 °C to temperatures above 100 °C during printing (Figure 1b). Such high temperatures (between 105 °C and 140 °C) can already cause annealing processes [13, 14], and eventually can facilitate the growth of β-crystals [15]. The observed peak at 148 °C corresponds to that of β-crystals found in literature [13], whereas the additional peak at 154 °C is referred to

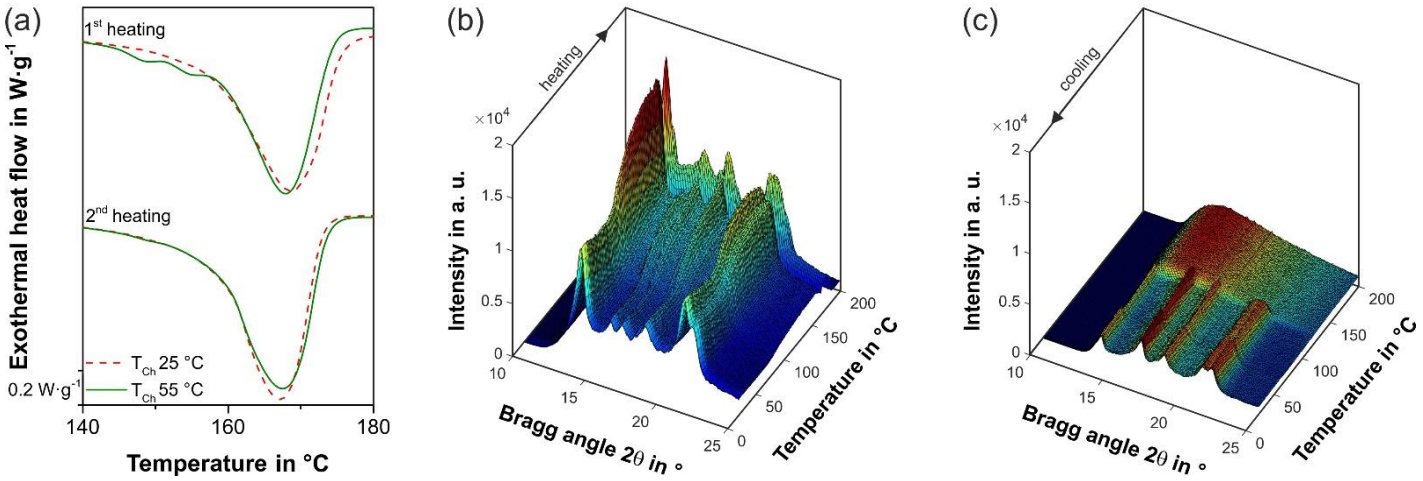

Figure 2: Representative DSC melting thermograms of the first and second heating cycle for the PP Charpy specimens printed at a chamber temperature T_{Ch} of 25 °C and 55 °C (a) and the in-situ X-ray diffraction patterns of the PP Charpy specimen printed at a T_{Ch} of 55 °C for a constant heating (b) and cooling (c).

the melting of β'-crystals, which most certainly formed in a recrystallisation step during the heating cycle of the DSC [16].

In order to verify the crystal modification, only the specimen printed at a T_{Ch} of 55 °C was analysed by means of in-situ XRD. The diffraction pattern between room temperature and roughly 150 °C (Figure 2b) clearly confirms the finding of the DSC. It proves that the material is both containing α- and β-crystals, as apart from the peaks corresponding to α-crystals (14.1°, 16.9°, 18.5°, 21.1° and 21.7°) also an extra peak at 16.1° and one intensified peak at 21.1°, corresponding to the (300) and (301) reflections of hexagonal β-crystals [17], are found [6]. Around 150 °C, a β-α-transition, similarly to Ref. [18] is observed, as the peaks at 16.1° and 21.1° steadily decrease and the peaks related to the α-crystals intensify until only the pattern of a typical α-crystal-dominated PP is visible around 155 °C. Beyond 170 °C, no distinct peaks are discernible, but scattering from the amorphous material, as all the crystals of PP are melted. During cooling (Figure 2c), the amorphous melt starts to form only α-crystals (Figure 2a) around 115 °C, which is in agreement with the DSC results [6]. No additional crystalline structures form during cooling. The clearly different overall and relative intensities of the diffraction peaks of the cooling step compared to the heating step can be related to differences in the probed sample volume due to melting [19]. Moreover, it can be explained by flow-induced orientations of the spherulites that originate from the FFF process, as after melting the process orientations occurring during 3D-printing are mainly annihilated and only a weak texture is developed [6, 19].

In order to verify whether process orientations are present in the investigated 3D-printed specimens, more polarised optical microscopy images were taken. Especially on regions that are exposed to high printing speeds, oriented spherulites in the shape of Shish-Kebab-structures that align along the printing direction were frequently found for both T_{Ch} (Figure 3a). As the thermal conductivity is dependent on flow-induced orientations and the anisotropy of crystals [20], this finding is additionally verified by thermal conductivity measurements on the same material. Depending on the printing orientation, the samples, in which the crystals are aligned in the measurement direction (in this set-up this equals to the 90° orientation [10]) show a 50% higher axial thermal conductivity than the samples, in which crystals are oriented perpendicularly to the measurement direction (0° orientation, Figure 3b). The specimens with a printing orientation of 0°/90° or ±45° lie between the two extremes of the 0° and 90° orientations. This finding proves that anisotropic crystals in the form of Shish-Kebab structures are formed during extrusion-based additive manufacturing of PP. This result and the presence of β-crystals has in turn positive effects on the tensile and bending properties of the printed material (please refer to Ref. [10]) as well as on the toughness [6].

4 CONCLUSIONS

In sum, the present study demonstrates the effect of an increased printing chamber temperature T_{Ch} on the microscopic, thermal and crystallographic properties of PP produced by extrusion-based additive manufacturing and therefore enables a deeper understanding of semi-crystalline 3D-printing materials. As the mean strand temperature during part production, obtained by in-situ thermography measurements, is significantly different for the two investigated T_{Ch}, the spherulites grow and nucleate in a different velocity, resulting in the double spherulite size for a T_{Ch} of 55 °C compared to that of 25 °C. Since the strands printed at a T_{Ch} of 55 °C are repeatedly exposed to temperatures over 105 °C, β-crystals are additionally formed among the dominant α-crystals, which was confirmed by DSC and in-situ

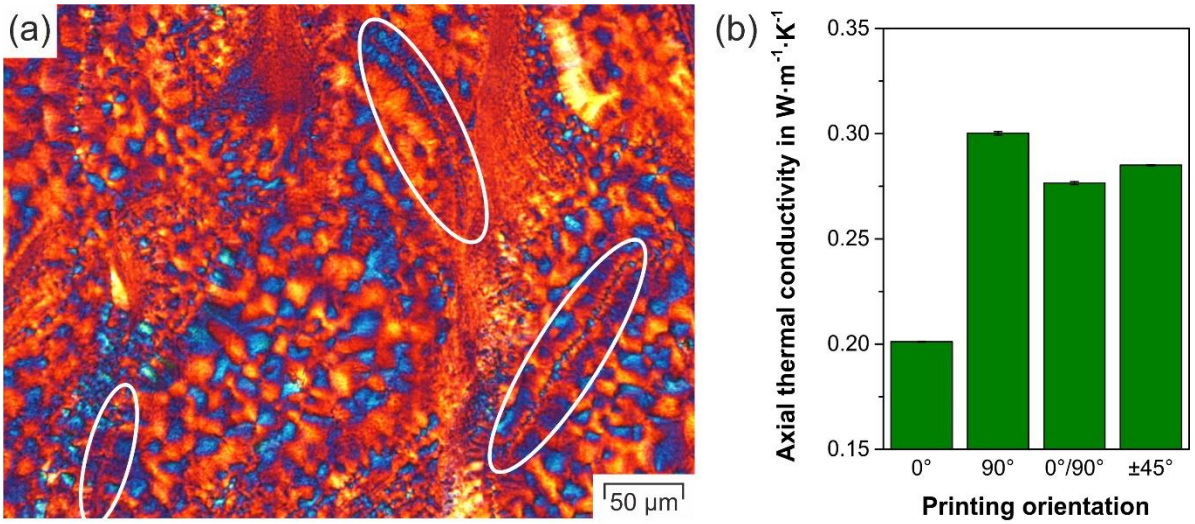

Figure 3: Polarised optical microscopy image of a microtome cut of an untested 3D-printed PP Charpy specimen that shows oriented crystals along the flow orientation (encircled in white) (a) and the axial thermal conductivity of neat 3D-printed PP as a function of the printing orientation (b).

XRD. In a concluding investigation, both on polarised optical microscopy and thermal conductivity measurements, orientations along the printing direction in the shape of Shish-Kebab structures were found. These orientations led to drastically altered relative and overall intensity levels in the XRD signal and to an increase of 50% in the thermal conductivity for the oriented crystals.

5 ACKOWLEDGEMENTS

This work was supported by the Austrian Research Promotion Agency (FFG) as part of the NextGen3D (Next Generation 3D, Grant Agreement No. 848624) and the AddManu (Grant Agreement No. 849297) project and by the doctoral scholarship of Ghent University (BOF16/FJD/014) for Martin Spoerk. Special thanks go to Maja Kuzmanović and Davy Deduytsche for the assistance in XRD measurements, and to Petra Erdely, Dr. Janak Sapkota and Dr. Joamin Gonzalez-Gutierrez for fruitful discussions.

6 REFERENCES

[1] Gibson, I.; Rosen, D.W.; Stucker, B.: Additive Manufacturing Technologies, 3D Printing, Rapid Prototyping, and Direct Digital Manufacturing, 2. Aufl., Springer, New York, 2015

[2] Carneiro, O.S.; Silva, A.F.; Gomes, R.: Fused deposition modeling with polypropylene 83, 2015, S. 768–776

[3] White, J.L.; Choi, D.D.: Polyolefins, Processing, Structure Development, and Properties, Hanser, München, 2005

[4] Spoerk, M.; Sapkota, J.; Weingrill, G., et al.: Shrinkage and Warpage Optimization of Expanded-Perlite-Filled Polypropylene Composites in Extrusion-Based Additive Manufacturing, Macromolecular Materials and Engineering (302), 2017, S. 1700143

[5] Wang, T.-M.; Xi, J.-T.; Jin, Y.: A model research for prototype warp deformation in the FDM process 33 (11-12), 2007, S. 1087–1096

[6] Spoerk, M.; Arbeiter, F.; Raguž, I., et al.: Polypropylene filled with glass spheres in extrusion-based additive manufacturing: Effect of filler size and printing chamber temperature, Macromolecular Materials and Engineering, 2018

[7] Costa, S.F.; Duarte, F.M.; Covas, J.A.: Estimation of filament temperature and adhesion development in fused deposition techniques 245, 2017, S. 167–179

[8] Ehrenstein, G.W.: Polymer Werkstoffe, Struktur - Eigenschaften - Anwendung, 3. Aufl., Carl Hanser Verlag GmbH & Co. KG, München, 2011

[9] Wang, L.; Gardner, D.J.: Effect of fused layer modeling (FLM) processing parameters on impact strength of cellular polypropylene 113, 2017, S. 74–80

[10] Spoerk, M.; Savandaiah, C.; Arbeiter, F., et al.: Anisotropic properties of oriented short carbon fibre filled polypropylene parts fabricated by extrusion-based additive manufacturing under review, 2018

[11] Wang, L.; Gramlich, W.M.; Gardner, D.J.: Improving the impact strength of Poly(lactic acid) (PLA) in fused layer modeling (FLM) 114, 2017, S. 242–248

[12] Lin, L.; Schlarb, A.K.: Vibration welding of nano-TiO 2 filled polypropylene 55 (2), 2015, S. 243–250

[13] Varga, J.: β-Modification of isotactic polypropylene, Preparation, structure, processing,

properties, and application 41 (4), 2002, S. 1121–1171
[14] O'kane, W.; Young, R.; Ryan, A.: The effect of annealing on the structure and properties of isotactic polypropylene films 34 (4), 1995, S. 427–458
[15] Bai, H.; Wang, Y.; Zhang, Z., et al.: Influence of Annealing on Microstructure and Mechanical Properties of Isotactic Polypropylene with β-Phase Nucleating Agent 42 (17), 2009, S. 6647–6655
[16] Fujiwara, Y.: Das Doppelschmelzverhalten der Beta-Phase des isotaktischen Polypropylens 253 (4), 1975, 273-282
[17] Cho, K.; Saheb, D.; Choi, J., et al.: Real time in situ X-ray diffraction studies on the melting memory effect in the crystallization of β-isotactic polypropylene 43 (4), 2002, S. 1407–1416
[18] Cho, K.; Nabi Saheb, D.; Yang, H., et al.: Memory effect of locally ordered α-phase in the melting and phase transformation behavior of β-isotactic polypropylene 44 (14), 2003, S. 4053–4059
[19] Spieß, L.; Teichert, G.; Schwarzer, R., et al.: Moderne Röntgenbeugung, 2. Aufl., Vieweg+Teubner, Wiesbaden, 2009
[20] Choy, C.L.; Chen, F.C.; Luk, W.H.: Thermal conductivity of oriented crystalline polymers, Journal of Polymer Science: Polymer Physics Edition 18 (6), 1980, S. 1187–1207